DOI: 10.1002/anie.200906283

Imaging Mass Spectrometry

Three-Dimensional Vizualization of Mouse Brain by Lipid Analysis Using Ambient Ionization Mass Spectrometry**

*Livia S. Eberlin, Demian R. Ifa, Chunping Wu, and R. Graham Cooks**

Two-dimensional (2D) imaging mass spectrometry (MS)[1] has emerged as a powerful technique in the biological sciences. It allows direct investigation of the distribution of a variety of lipids, drugs, biological defensive agents, pigments, and proteins in plant and animal tissues with high specificity and without the need of fluorescent or radioactive labeling normally used in histochemical protocols.[2,3] In imaging MS, the chemical identity of molecules present on a surface is investigated as a function of their 2D spatial distribution (x and y coordinates).

Three-dimensional (3D) images can be constructed from a suitable set of 2D data, and they illustrate the spatial distributions of specific biomolecules in substructures of tissues, including pathological features.[4] Two basic approaches, depth profiling and serial sectioning, have been described for recording the information needed to create 3D MS-based images. In depth-profiling experiments, a desorbing agent is used to remove shallow layers of material from the surface of the object in between the recording of surface analysis data. Secondary-ion mass spectrometry (SIMS),[5] laser ablation electrospray ionization (LAESI),[2,6] and laser ablation flowing atmospheric-pressure afterglow (LA-FAPA)[7] are ionization techniques that have been used to create 3D MS models by depth profiling. In the alternative serial-sectioning approach, serial sections of the object are obtained through mechanical sectioning and individually analyzed. Matrix-assisted laser desorption ionization (MALDI) MS[8] is the only technique that has been used for serial-sectioning analysis in 3D imaging.

SIMS and MALDI are well-established techniques that have been widely used for molecular imaging under vacuum but newer ambient ionization methods such as desorption electrospray ionization (DESI),[9,10] LAESI, atmospheric-pressure infrared (AP-IR) MALDI and LA-FAPA allow the direct analysis of samples in the open atmosphere. In particular, DESI-MS is an ambient desorption ionization method with the advantages of little or no sample preparation, ease of implementation, and simplified analysis.[11] Most importantly, the problem of endogenous compounds' dislocation during the sample-preparation procedures of standard histochemical analysis can be overcome, because tissue sections are analyzed directly outside the mass spectrometer without any further treatment after sectioning. It has been shown that DESI-MS imaging can be used to distinguish between cancerous and non-cancerous tissue samples using multiple marker lipids.[12] DESI-MS imaging has also been applied to measure the distributions of drugs and their metabolites in tissue.[13] Low-polarity compounds can be imaged using reactions with selective reagents added to the spray.[14] Herein, we report on 3D molecular image construction by desorption electrospray ionization (DESI). To test this capability, high-quality 2D DESI-MS ion images from coronary sections of mouse brain were used to build a 3D image which then allows direct correlation and easy visualization of endogenous compounds in substructures of the brain.

To obtain the high-quality 2D images essential to building reliable 3D images, experimental conditions were optimized to maximize the signal intensity and increase image quality (see the Supporting Information for experimental details). Indeed, it has been shown that several experimental parameters can be optimized to improve the quality of DESI data.[9,15]

Two distinctive MS peak patterns were observed in the negative-ion mode for the brain sections analyzed depending on the region of the brain under investigation (Figure 1). The differences are associated with the lipid compositions representative of the gray and white matter of the brain. The majority of the ions observed in the mass spectra correspond to deprotonated free fatty acids, phosphatidylserines (PS), phosphatidylinositols (PI), and sulfatides (ST), with PS 18:0/22:6 being the major lipid found in the gray matter and ST 24:1 the major lipid found in the white matter. Lipid assignments were confirmed by tandem mass spectrometry (MS/MS) through comparisons to literature data.[16] Table S1 in the Supporting Information lists the major peaks detected in the mouse brain in the negative-ion mode and tabulates the corresponding set of fragment ions generated from each precursor ion in the course of MS/MS analysis.

Two-dimensional ion images of specific lipid species observed in the mouse brain tissue are shown in Figure S1 in the Supporting Information. For all sections analyzed, distinctive and complementary spatial distributions were observed. The most abundant ions in the mass spectra, m/z 834.4 and m/z 888.8, were identified as PS 18:0/22:6 and ST 24:1, respectively. The ion image of PS 18:0/22:6 shows a homogeneous distribution of this lipid in the brain gray matter (Figure 1c, in green), while lipid ST 24:1 is distributed homogenously in the white matter (Figure 1d, in red). Similar lipid distributions have been reported previously for rat brain.[10] To implement 3D imaging, these two lipids were

[*] L. S. Eberlin, Dr. D. R. Ifa, C. Wu, Prof. R. G. Cooks
Department of Chemistry, Purdue University
West Lafayette, IN 47907 (USA)
Fax: (+1) 765-494-9421
E-mail: cooks@purdue.edu

[**] This work was supported by the U.S. National Institutes of Health (grant 1R21EB009459-01).

Supporting information for this article is available on the WWW under http://dx.doi.org/10.1002/anie.200906283.

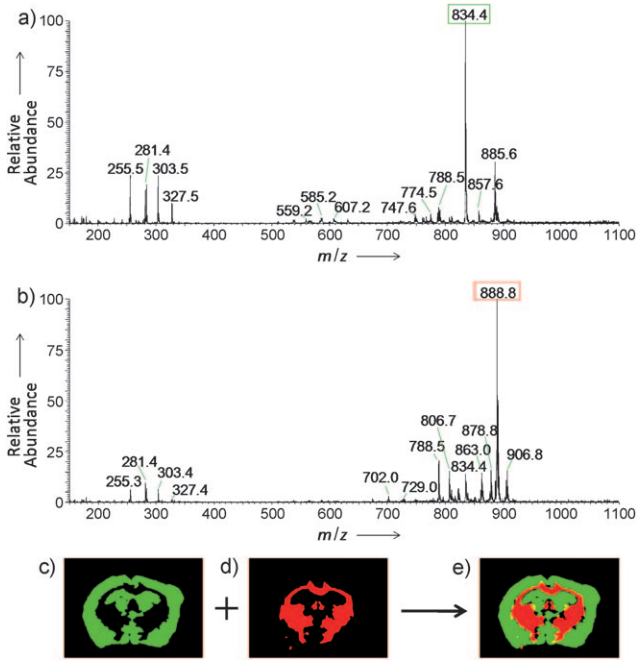

Figure 1. DESI mass spectrum obtained from a 20 μm thick mouse brain coronal section at Bregma: −1.060 mm in the a) gray-matter and b) white-matter region. The coronal sections were referenced to a stereotaxic coordinate where the zero coordinate is the Bregma (the point of junction of the sagittal and coronal sutures on the cranium). The most intense ion present in the gray matter at *m/z* 834.4 was identified as PS 18:0/22:6. In the white matter, the most intense ion at *m/z* 888.8 was identified as ST 24:1. DESI-MS ion image is shown in green for PS 18:0/22:6 (c) and in red for ST 24:1 (d). The overlaid ion images obtained (e) are used to construct the 3D model.

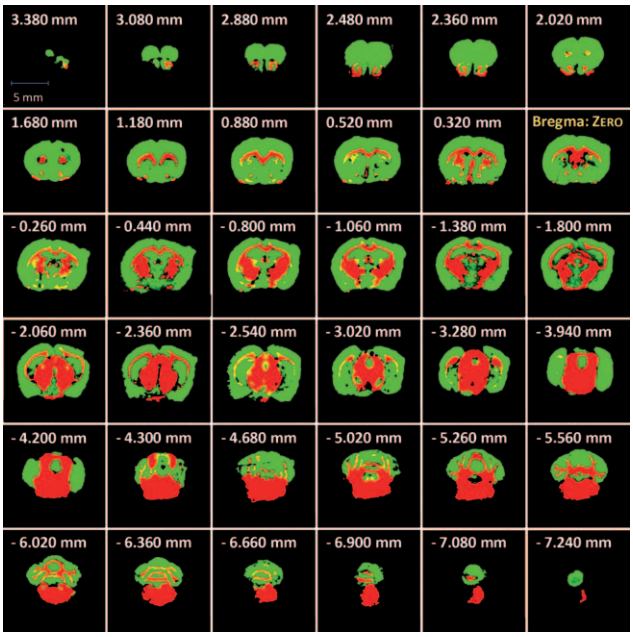

Figure 2. Thirty-six 2D overlaid ion images of the lipids PS 18:0/22:6 (green) and ST 24:1 (red) used to render a 3D model of the mouse brain. The 2D images span the mouse brain from Bregma 3.380 to −7.240 mm.

mapped in three dimensions; each nominal mass represents a group of lipids mainly seen in the gray- or white-matter regions of the brain. Mapping only the lipid signals is an approximation since it disregards structures of the brain in which these lipids are not present.

The 2D ion images used to construct the 3D model are made up of an overlay of the distribution of lipids PS 18:0/22:6 and ST 24:1 (Figure 1e). The contrast used in displaying the images was increased to allow better visualization of distinctive areas of the brain. This was also necessary because the software used for the construction of the 3D volumes segments the brain based on color differences. The 36 overlaid ion images used for the 3D model are shown in Figure 2. Several anatomical structures of the mouse brain can be observed in the 2D tissue sections showing the distributions of PS 18:0/22:6 and ST 24:1. For instance, in slice Bregma: 1.180 mm, the distribution of ST 24:1 reveals such anatomic structures as the forceps minor of the corpus callosum, anterior commissure, lateral olfactory tract, and striatum (Figure S2 in the Supporting Information). While several structures of the brain can be observed in the 36 individual 2D sections analyzed by DESI-MS imaging, a full view of these structures in the total brain volume can be achieved only through the construction of the 3D brain model. By adding the dimension of depth to the total image a better visualization of the object volume and the relative positions of its structures in space is achieved.

Three-dimensional models of the mouse brain were constructed using Able Software 3D-Doctor (see the Supporting Information). The correct scale in all three dimensions was obtained by providing the software with the physical dimensions of the 2D images and calibrating the 2D images using its pixel size (*x* and *y* dimensions). The same colors as those used for the 2D images for PS 18:0/22:6 and ST 24:1 were used in the 3D model. The maximum number of surface polygons was selected such that smoothing was minimized to avoid distortion in the brain model.

The 3D image obtained from the 36 2D ion images is a simplified representation of the mouse brain, in fact a model of the actual object. Approximations used for building the 3D image included selecting a total of 36 sections out of the 560 obtained and assuming that there is no sudden change in molecular distribution between two adjacent sections. Therefore, the trade-off between image quality and time has to be considered in the construction of 3D models. It was found that a high-quality 3D model with extensive structural information could in fact be constructed by using the 36 sections analyzed. A total analysis time of approximately 40 h was required to image the 36 sections used to render the 3D model. The 3D construction of the distribution of lipids PS 18:0/22:6 (green) and ST 24:1 (red) throughout the mouse brain is shown from different views in Figure 3. For this chosen case in which the selected lipids present a complementary distribution covering the majority of the brain, the overlaid 3D model obtained is a representation of the whole brain (Figure 3d,e). However, separate views showing the distribution of a single lipid can also be selected. Figure 3a shows the distribution of PS 18:0/

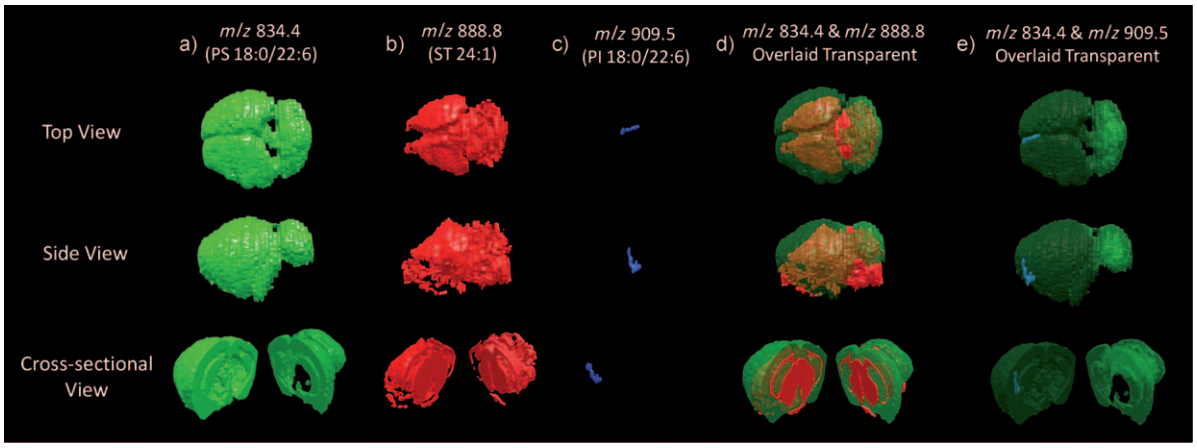

Figure 3. 3D models of the mouse brain by DESI-MS. Top, side, and cross-sectional views are shown for the 3D construction of the distribution of a) PS 18:0/22:6 in green, b) ST 24:1 in red, and c) PI 18:0/22:6 in blue. The same views are shown for the transparent overlaid distributions of the lipids d) PS 18:0/22:6 and ST 24:1, and e) PS 18:0/22:6 and PI 18:0/22:6.

22:6 throughout the brain, and this allows a full visualization of the gray-matter region in the total volume of the brain to be obtained. In contrast, the 3D visualization of the distribution of ST 24:1 represents the white-matter region of the brain and also shows a complete view of substructures, such as the corpus callosum and anterior commissure, throughout the brain volume (Figure 3b). The quality of these 3D images will be tested in future use. Cross-sectional views of the 3D models can be used to investigate substructures in specific parts of the brain. (Additional visualizations of the overlaid and separated distribution of the lipids selected are shown in Figure S3 in the Supporting Information.)

In addition, endogenous molecules with distinctive distributions in three dimensions can be easily visualized, allowing direct correlation to substructures of the mouse brain. For example, a 3D model obtained for *m*/*z* 909.5 (Figure 3c), identified as PI 18:0/22:6 (see tandem MS in Figure S4a in the Supporting Information), shows that this lipid is observed exclusively in a small region at the frontal part of the brain spanning Bregma: 2.020 to Bregma: 3.380 mm (Figure S5 in the Supporting Information). An overlaid image with PS 18:0/22:6 is shown in Figure 3e for better visualization of the distribution of this lipid within the brain volume. Further investigation revealed that this region of the brain presents a unique lipid profile in which the relative intensity of the polyunsaturated fatty acid docosohexaenoate 22:6 (DHA, *m*/*z* 327.4) in relation to the monounsaturated fatty acid 18:1 (*m*/*z* 281) is considerably increased compared to the lipid profile in the white matter of the brain (Figure S4b in the Supporting Information). Moreover, several other phospholipids besides PI 18:0/22:6, such as PS 16:0/22:6 (*m*/*z* 806.4) and PE 16:0/22:6 (*m*/*z* 746.5), with high polyunsaturated fatty content were exclusively observed in this region. Comparisons between the ion images obtained within this region and reference sections[17] indicates that this unique lipid distribution is associated with the lipid composition of the granule cells from the glomerular layer of the olfactory bulb (Figure S4c,d in the Supporting Information). These results agree with the reported high levels of polyunsaturated phospholipids observed in the olfactory tissue.[18]

The results reported here represent the first 3D molecular reconstruction of mouse brain by DESI-MS imaging. Different lipids detected in the negative-ion mode mapped two-dimensionally are used to build 3D models of a mouse brain. A trade-off between image quality and time was considered in the construction of the 3D models as well as approximations that could limit resolution and information. Nevertheless, the methodology has the potential to provide comprehensive information on the 3D distribution of molecules of interest, and it allows direct correlations between these molecules and the substructures of the brain. This should be a valuable step in understanding the biochemical processes that occur in the organ. This method is applicable to the analysis of the distribution of lipids in any other organ that can be examined using 2D sections. Furthermore, the images and models obtained by DESI-MS can be correlated to proteomic MALDI-MS data, providing knowledge on the connection between the distributions of different classes of molecules in organs. We anticipate that the field of histochemical analysis by imaging MS with contributions of DESI-MS and other MS techniques will permit the creation of a mass-spectrometry-based biomolecular atlas for mouse brain and other animal organs.

Received: November 7, 2009
Published online: December 29, 2009

Keywords: imaging techniques · ionization · mass spectrometry · phospholipids · tissue analysis

[1] M. L. Pacholski, N. Winograd, *Chem. Rev.* **1999**, *99*, 2977; L. A. McDonnell, R. M. A. Heeren, *Mass Spectrom. Rev.* **2007**, *26*, 606; E. H. Seeley, R. M. Caprioli, *Proteomics Clin. Appl.* **2008**, *2*, 1435; S. G. Boxer, M. L. Kraft, P. K. Weber, *Annu. Rev. Biophys.* **2009**, *38*, 53.
[2] P. Nemes, A. A. Barton, A. Vertes, *Anal. Chem.* **2009**, *81*, 6668.

[3] A. L. Lane, L. Nyadong, A. S. Galhena, T. L. Shearer, E. P. Stout, R. M. Parry, M. Kwasnik, M. D. Wang, M. E. Hay, F. M. Fernandez, J. Kubanek, *Proc. Natl. Acad. Sci. USA* **2009**, *106*, 7314.
[4] T. K. Sinha, S. Khatib-Shahidi, T. E. Yankeelov, K. Mapara, M. Ehtesham, D. S. Cornett, B. M. Dawant, R. M. Caprioli, J. C. Gore, *Nat. Methods* **2008**, *5*, 57.
[5] T. L. Colliver, C. L. Brummel, M. L. Pacholski, F. D. Swanek, A. G. Ewing, N. Winograd, *Anal. Chem.* **1997**, *69*, 2225; S. G. Ostrowski, C. T. Van Bell, N. Winograd, A. G. Ewing, *Science* **2004**, *305*, 71.
[6] P. Nemes, A. Vertes, *Anal. Chem.* **2007**, *79*, 8098.
[7] J. T. Shelley, S. J. Ray, G. M. Hieftje, *Anal. Chem.* **2008**, *80*, 8308.
[8] R. M. Caprioli, T. B. Farmer, J. Gile, *Anal. Chem.* **1997**, *69*, 4751; P. Chaurand, S. A. Schwartz, D. Billheimer, B. G. J. Xu, A. Crecelius, R. M. Caprioli, *Anal. Chem.* **2004**, *76*, 1145.
[9] D. R. Ifa, J. M. Wiseman, Q. Y. Song, R. G. Cooks, *Int. J. Mass Spectrom.* **2007**, *259*, 8.
[10] J. M. Wiseman, D. R. Ifa, Q. Y. Song, R. G. Cooks, *Angew. Chem.* **2006**, *118*, 7346; *Angew. Chem. Int. Ed.* **2006**, *45*, 7188.
[11] R. G. Cooks, Z. Ouyang, Z. Takats, J. M. Wiseman, *Science* **2006**, *311*, 1566.
[12] A. L. Dill, D. R. Ifa, N. E. Manicke, A. B. Costa, J. A. Ramos-Vara, D. W. Knapp, R. G. Cooks, *Anal. Chem.* **2009**, *81*, 8758.
[13] V. Kertesz, G. J. Van Berkel, M. Vavrek, K. A. Koeplinger, B. B. Schneider, T. R. Covey, *Anal. Chem.* **2008**, *80*, 5168; J. M. Wiseman, D. R. Ifa, Y. X. Zhu, C. B. Kissinger, N. E. Manicke, P. T. Kissinger, R. G. Cooks, *Proc. Natl. Acad. Sci. USA* **2008**, *105*, 18120.
[14] C. Wu, D. R. Ifa, N. E. Manicke, R. G. Cooks, *Anal. Chem.* **2009**, *81*, 7618.
[15] T. J. Kauppila, N. Talaty, P. K. Salo, T. Kotiah, R. Kostiainen, R. G. Cooks, *Rapid Commun. Mass Spectrom.* **2006**, *20*, 2143; S. P. Pasilis, V. Kertesz, G. J. Van Berkel, *Anal. Chem.* **2007**, *79*, 5956.
[16] F. Gao, X. K. Tian, D. W. Wen, J. Liao, T. Wang, H. W. Liu, *Biochim. Biophys. Acta Mol. Cell Biol. Lipids* **2006**, *1761*, 667; F. F. Hsu, J. Turk, *J. Am. Soc. Mass Spectrom.* **2001**, *12*, 1036; M. Pulfer, R. C. Murphy, *Mass Spectrom. Rev.* **2003**, *22*, 332; N. E. Manicke, J. M. Wiseman, D. R. Ifa, R. G. Cooks, *J. Am. Soc. Mass Spectrom.* **2008**, *19*, 531.
[17] K. B. J. Franklin, G. Paxinos, *The Mouse Brain in Stereotaxic Coordinates*, Compact 3rd ed., Academic Press, New York, **2008**.
[18] S. L. Niu, D. C. Mitchell, B. J. Litman, *J. Biol. Chem.* **2001**, *276*, 42807; Y. Russell, P. Evans, G. H. Dodd, *J. Lipid Res.* **1989**, *30*, 877.

